Zwitterionic Acceptor Moieties: Small Reorganization Energy and Unique Stabilization of Charge Transfer Products†

Dirk M. Guldi,*,‡ Chuping Luo,‡ Nicholas A. Kotov,*,§ Tatiana Da Ros,|| Susanna Bosi,|| and Maurizio Prato*,||

Radiation Laboratory, University of Notre Dame, Notre Dame, Indiana 46556, Chemistry Department, Oklahoma State University, Stillwater, Oklahoma, 74078, and Dipartimento di Scienze Farmaceutiche, Università di Trieste, Piazzale Europa, 1, 34127 Trieste, Italy

Received: September 18, 2002

A series of fulleropyrrolidine- and fulleropyrrolidinium-based donor−acceptor ensembles were tested in light of intrinsic reorganization energies for photoinduced electron transfer events. Among these complexes, the fulleropyrrolidinium ions are particularly well-suited for the role of an acceptor moiety. In fact, once reduced, fulleropyrrolidinium ions exhibit a zwitterionic character, due to the contemporary presence of a positive pyrrolidinium ion together with the fullerene radical ion. We demonstrate that this zwitterionic character of the acceptor plays a central role in improving acceleration of charge separation and deceleration of charge recombination. While the charge separation occurs with dynamics close to the top region of the Marcus parabola, the charge recombination rates are pushed deeply into the inverted region of the parabolic dependence. Overall, we determined reorganization energies (λ) for the fulleropyrrolidinium-based ensemble that are appreciably smaller than those seen for the fulleropyrrolidine-based analogue, while keeping the electronic coupling element constant (!). Remarkable is the oxygen effect on the zwitterionic fulleropyrrolidinium acceptor—not seen on the fulleropyrrolidine acceptor—in the charge-separated radical pair.

Introduction

Electron transfer is one of the prototypical chemical reactions and plays by itself a fundamental role in respiration, photosynthesis, and redox reactions in intermediary metabolism. Essentially, it involves proteins with redox centers that are separated by relatively long distances. As such, a complete understanding of natural electron transfer requires a multidisciplinary approach that focuses on a series of physical and kinetic parameters in simpler model systems of light harvesting arrays and reaction centers. In this context, a large body of work—performed in recent years—demonstrated that C_{60} emerged as a promising building block for devising molecular electron transfer models. In particular, integration of C_{60}—a three-dimensional (3D) electron acceptor—holds great expectations in electron transfer reactions, which is in large due to its small reorganization energy in light-induced charge separation processes.[2] The delocalization of charges, which can be either electrons or holes, within the carbon framework together with the rigid, confined structure of the aromatic π-sphere are beneficial for the stabilization of charged entities.[3]

The role of different electron donors, covalently linked to the reactive carbon framework of C_{60}, has been thoroughly investigated,[4] while only a few scattered reports can be found that focus on the modification of the acceptor properties of the fullerene core.[5−8] Among the relatively few examples, relevant contributions comprise the work on integrating C_{70} or, more recently, $C_{59}N$—both being slightly better electron acceptors than C_{60}—into photoactive charge transfer materials.[6,7]

SCHEME 1

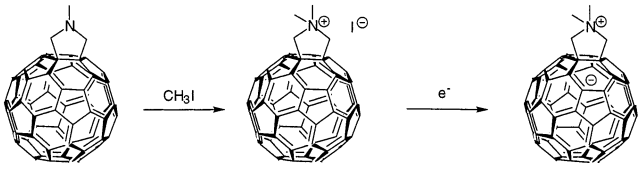

Fulleropyrrolidinium ions are photostable C_{60} derivatives that show better electron acceptor features not only than fulleropyrrolidines but also than pristine C_{60}.[8] In addition, their inclusion in a donor−acceptor dyad would give rise to a stable singly reduced species, due to the zwitterionic nature of this intermediate (Scheme 1).[9]

These properties render fulleropyrrolidinium ions particularly attractive tools for efficient conversion of solar energy. In fact, variation of the fullerene acceptor features in donor−acceptor ensembles is attained, by simply exchanging the parent fulleropyrrolidine with a fulleropyrrolidinium moiety via methylation of the pyrrolidine nitrogen (Scheme 1).

In the present work, the synthesis of a series of C_{60}−Fc donor−acceptor dyads is reported. This allowed us to probe the effects stemming from (i) flexible vs rigid donor−acceptor linkages, (ii) electronic changes of the electron-donating ferrocene moiety, and (iii) far more important changes of the fullerene acceptor, that is, testing a fulleropyrrolidine vs fulleropyrrolidinium core, on charge separation and charge recombination in C_{60}−Fc ensembles. In addition, we present the first comprehensive assay of λ-values for intramolecular electron transfer involving different C_{60} acceptors.

† Part of the special issue "Arnim Henglein Festschrift".

* To whom correspondence should be addressed. D.M.G.: Tel: 1 574 631 7441. Fax: 1 574 631 8068. E-mail: guldi.1@nd.edu. N.A.K.: Tel: 1 405 744 3991. Fax: 1 405 744 6007. E-mail: kotov@okstate.edu. M.P.: Tel: 39 040 558 7883. Fax: 39 040 52572. E-mail: prato@univ.trieste.it.

‡ University of Notre Dame.

§ Oklahoma State University.

|| Università di Trieste.

10.1021/jp0220938 CCC: $25.00
Published on Web 03/19/2003

Experimental Section

Fullerene derivatives **3**−**8** were prepared according to published work. The 6-(carboxymethyl-amino)hexanoic acid *tert*-butyl ester **9**[10] and the ferrocene methylamine **12**[11] were prepared according to previous reports. Electrospray mass spectra (ES-MS) were taken from tetrahydrofuran (THF)−MeOH 1:1 solutions.

Preparation of Ester 10. A solution of C_{60} (1 g, 1.39 mmol), 6-(carboxymethyl-amino)hexanoic acid *tert*-butyl ester (370 mg, 1.39 mmol), and paraformaldehyde (210 mg, 7 mmol) in 500 mL of toluene was refluxed at 110 °C for 2 h. The solvent was evaporated in a vacuum, and the residue was cromatographed on silica gel (eluant pure toluene and Tol/AcOEt 9:1). The product was dissolved in methylene chloride and precipitated by addition of methanol as a dark brown solid; 370 mg, yield 28.5%; $C_{72}H_{23}NO_2$ MW 933.99. ^{1}H NMR ($CDCl_3$): δ 4.37 (s, 4H), 3.07 (t, 2H, J = 6.96), 2.33 (t, 2H, J = 6.96), 2.05−1.41 (m, 6H), 1.46 (s, 9H). ^{13}C NMR ($CDCl_3$): δ 173.16, 155.12, 147.32, 146.25, 146.12, 146.07, 145.42, 145.31, 144.59, 143.11, 142.64, 142.27, 142.09, 141.91, 140.17, 136.27, 80.20, 70.77, 68.13, 55.03, 35.72, 29.84, 28.80, 28.32, 27.32, 25.27. ES-MS 933 (M^+).

Hydrolysis of Ester 10 and Preparation of Acid 11. To a solution of **10** (300 mg, 0.32 mmol) in 100 mL of dichloromethane, 10 mL of trifluoroacetic acid was added. After 16 h, the solvent was evaporated and the solid residue was washed several times with ethyl ether to give 280 mg (yield 98%) of a dark brown solid; $C_{68}H_{15}NO_2$ MW 877.88. ES-MS 877 (M^+). IR (KBr): 2926, 1692, 1530, 1187.

Preparation of Pyrrolidine Dyad 1. To a suspension of acid **11** (50 mg, 0.057 mmol) in 20 mL of anhydrous dichloromethane, bromotripyrrolidinophosphonium hexafluorophosphate (PBrOP) (53 mg, 0.114 mmol) and a catalytic amount of dimethyl amino pyridine were added. After 20 min, a solution of ferrocene methylamine (50 mg, 0.114 mmol) in 5 mL of dichloromethane was added dropwise. After 4 h, the solution was filtered and chromatographed on an alumina column (eluant Tol/i-PrOH 9/1) after evaporation of the solvent. The product was dissolved in methylene chloride and precipitated by addition of methanol to give 48 mg of a dark brown solid (78%); $C_{79}H_{26}FeN_2O$, MW 1074.95. ^{1}H NMR ($CDCl_3$): δ 5.62 (bs, 1H), 4.39 (s, 4H), 4.23−4.06 (m, 9H), 3.07 (t, 2H, J = 8.42), 3.47 (t, 2H, J = 8.42), 2.04−1.72 (m, 6H), 1.56 (s, 9H). ^{13}C NMR ($CDCl_3$): δ 172.22, 115.10, 147.32, 146.25, 146.12, 146.07, 145.42, 144.58, 142.65, 142.08, 141.90, 140.17, 136.24, 134.12, 70.75, 69.75, 68.71, 68.46, 68.44, 68.41, 68.35. ES-MS 1074 (M^+). IR (KBr): 2932, 1644, 1530, 1009, 811. UV (THF): λ_{max} 430 nm, 705 nm.

Preparation of Pyrrolidinium Dyad 2. A solution of **1** (50 mg, 0.046 mmol) in 1 mL of methyl iodide was stirred at 60 °C for 16 h in a screw cap vial. After the excess reagent was evaporated, the residue was washed several times with ethyl ether to give 56 mg (99%) of a dark brown solid; $C_{80}H_{29}FeIN_2O$, MW 1216.89. ES-MS 1088 (M^+).

Photophysics. Picosecond laser flash photolysis experiments were carried out with 355 nm laser pulses from a mode-locked, Q-switched Quantel YG-501 DP Nd:YAG laser system (pulse width 18 ps, 2−3 mJ/pulse). Nanosecond laser studies were performed with laser pulses from a Molectron UV-400 nitrogen laser system (337.1 nm, 8 ns pulse width, 1 mJ/pulse). The photomultiplier output was digitized with a Tektronix 7912 AD programmable digitizer.

Fluorescence lifetimes were measured with a Laser Strope Fluorescence Lifetime Spectrometer (Photon Technology International) with 337 nm laser pulses from a nitrogen laser fiber-coupled to a lens-based T-formal sample compartment equipped with a stroboscopic detector. Details of the Laser Strobe systems are described on the manufacture's web site: http://www.pti-nj.com.

Emission spectra were recorded with a SLM 8100 spectrofluorometer. The experiments were performed at room temperature. Each spectrum represents an average of at least five individual scans, and appropriate corrections were applied whenever necessary.

SCHEME 2

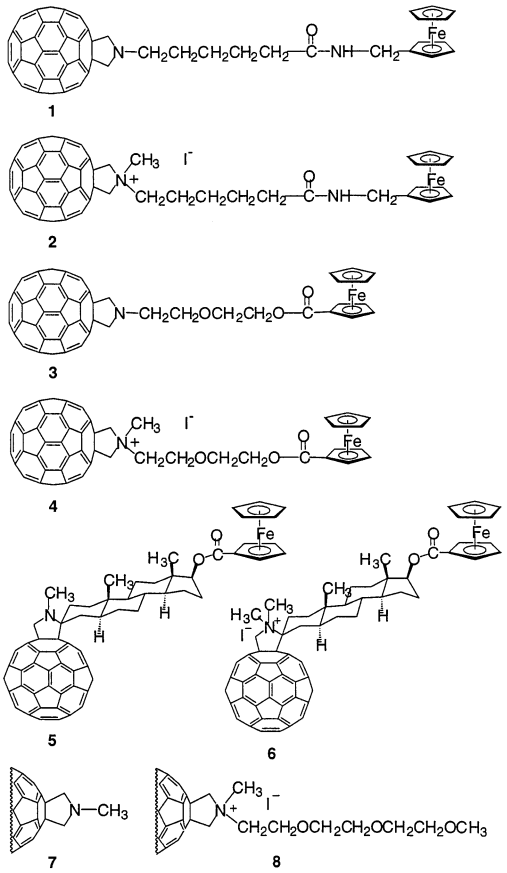

SCHEME 3

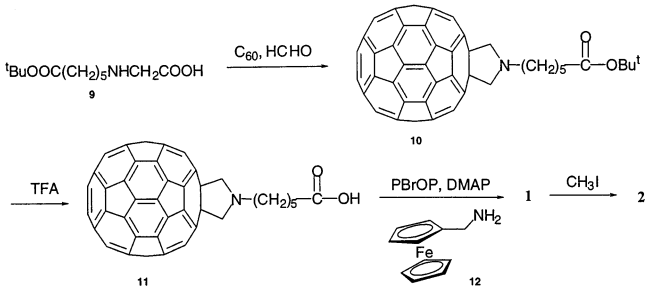

Results and Discussion

Synthesis. The structure of the compounds studied in this work is reported in Scheme 2. While the synthesis of derivatives **3**−**8** has already been reported, compounds **1** and **2** were prepared according to Scheme 3. The synthesis of neutral dyad **1** was obtained by the known 1,3-dipolar cycloaddition of azomethine ylides to C_{60}.[12] In this case, N-functionalized glycine **9** was allowed to react with paraformaldehyde to obtain fulleropyrrolidine **10**. The ester function was deprotected, and

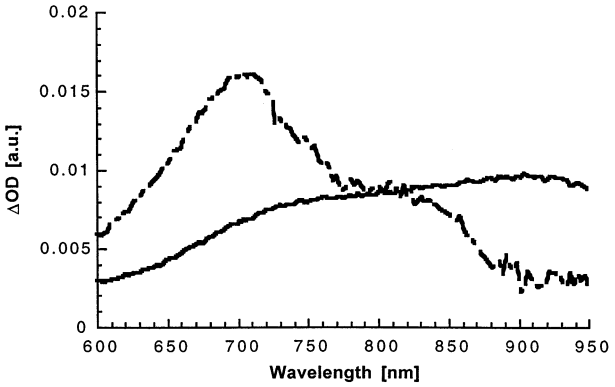

Figure 1. Differential absorption spectra (visible and near-infrared) obtained upon picosecond flash photolysis (355 nm) of ~1.0×10^{-5} M solutions of fulleropyrrolidine **7** in nitrogen-saturated toluene with a time delay of 50 (solid spectrum) and 5000 ps (dashed spectrum), showing the singlet and triplet excited state features of photoexcited fulleropyrrolidine **7**.

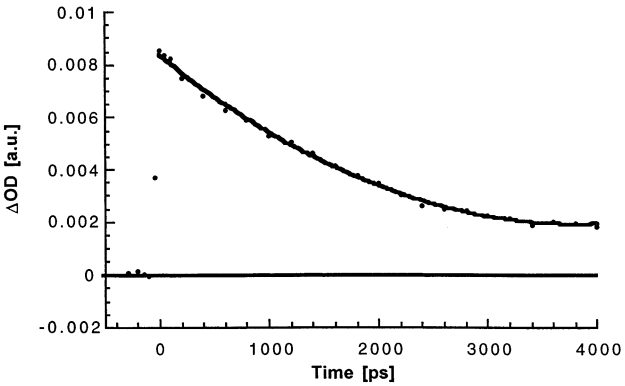

Figure 2. Time−absorption profiles at 880 nm monitoring the fullerene ISC dynamics in photoexcited fulleropyrrolidine **7**.

the resulting free acid was condensed with ferrocene amine **12** to give dyad **1**. The latter was alkylated with methyl iodide to afford the desired pyrrolidinium ion **2** (Scheme 3).

Photophysics. To characterize the charge transfer behavior of dyads **1**−**6**, transient absorption measurements, following 18 ps or 8 ns laser pulses, were conducted in several solvents and compared to those of fulleropyrrolidine **7** and fulleropyrrolidinium salt **8**. In addition, complementary sets of steady state and time-resolved fluorescence spectroscopy experiments were carried out to shed further light onto the fullerene singlet excited state deactivation.

In the two references, fulleropyrrolidine **7** and fulleropyrrolidinium salt **8**, the photophysics of the fullerene singlet excited state are governed by slow (5×10^8 s^{-1}) but efficient (~100%) intersystem crossing (ISC) dynamics to the triplet manifold.[9] Spectroscopically, strong transitions in the near-infrared (i.e., singlet−singlet absorption at 880 nm) and visible (i.e., triplet−triplet absorption at 700 nm) help to identify the two excited states—see Figure 1.[9] The dynamics of the ISC processes in **7** and **8** are nearly solvent-independent, since the energies of the singlet and triplet excited states remain virtually unchanged. An illustration is given in Figure 2. It should be noted that since the C_{60} moieties in dyads **1**−**6** act as photoexcited chromophores, the singlet excited state energies of **7** and **8**—as derived from the weakly fluorescing *0−0 maxima ($\Phi = 6.0 \times 10^{-4}$)—are 1.73 and 1.76 eV, respectively.

Upon photoexciting the C_{60} core in dyads **1**−**6** with short 355 nm laser pulses, the same singlet excited state absorptions of ^{1}*C_{60} were found around 880 nm. In most cases, the decays

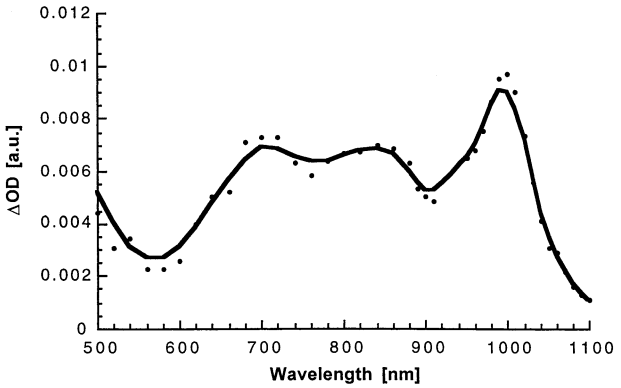

Figure 3. Differential absorption spectrum (visible and near-infrared) obtained upon nanosecond flash photolysis (337 nm) of ~1.0×10^{-5} M solutions of dyad **6** in nitrogen saturated *ortho*-dichlorobenzene with a time delay of 50 ns at room temperature.

TABLE 1: Charge Separation and Recombination Kinetics in C_{60}−Fc Dyads 1−4

		toluene	THF	benzonitrile	DMF
dyad **1**	k_{CS} (s^{-1})	1.7×10^9	1.8×10^9	1.9×10^9	2.0×10^9
	Φ_{FL}	2.2×10^{-6}	2.1×10^{-6}	2.0×10^{-6}	1.7×10^{-6}
	k_{CR} (s^{-1})			7.7×10^6	
dyad **2**	k_{CS} (s^{-1})		2.8×10^9	3.4×10^9	4.0×10^9
	Φ_{FL}		1.5×10^{-6}	1.4×10^{-6}	1.2×10^{-6}
	k_{CR} (s^{-1})			6.6×10^6	
dyad **3**	k_{CS} (s^{-1})	1.7×10^9	1.9×10^9	2.0×10^9	2.2×10^9
	Φ_{FL}	2.0×10^{-6}	1.9×10^{-6}	1.6×10^{-6}	1.4×10^{-6}
	k_{CR} (s^{-1})			9.5×10^6	
dyad **4**	k_{CS} (s^{-1})		2.1×10^9	2.3×10^9	2.6×10^9
	Φ_{FL}		1.6×10^{-6}	1.5×10^{-6}	1.4×10^{-6}
	k_{CR} (s^{-1})			9.1×10^6	

TABLE 2: Charge Separation and Recombination Kinetics in C_{60}−Androstane−Fc Dyads 5 and 6

dyad	solvent	charge separation (s^{-1})	charge recombination (s^{-1})	k_{CS}/k_{CR} ratio	$-\Delta G_{CR}°$ (eV)
5	toluene		triplet		
	ortho-dichloro-benzene	8.9×10^8	9.3×10^5	964	1.11
	benzonitrile	1.0×10^9	1.2×10^6	879	1.07
	DMF	1.4×10^9	2.8×10^6	493	0.98
6	*ortho*-dichloro-benzene	1.5×10^9	6.2×10^5	2340	0.94
	benzonitrile	1.4×10^9	1.0×10^6	1322	0.9
	DMF	1.5×10^9	2.0×10^6	735	0.81

were notably faster than in **7** and **8** (see below). Furthermore, characteristic bands in the near-infrared that are centered around 1000 nm and are ascribed to the fullerene radical anion, $C_{60}^{\bullet-}$, see Figure 3, appeared concomitantly with the ^{1}*C_{60} decay. This leads to the assumption that in the investigated donor−acceptor systems intramolecular electron transfer events control the transformation of the ^{1}*C_{60}−Fc precursor into the $C_{60}^{\bullet-}$−Fc^+ product.[13] The maxima at 400 and 1000 nm are clearly attributed to $C_{60}^{\bullet-}$, while the weak absorption of Fc^+ with an extinction coefficient of ~500 M^{-1} cm^{-1} at 625 nm is masked by the much stronger absorption (>5000 M^{-1} cm^{-1}) of $C_{60}^{\bullet-}$ in this region. By fitting the rise and decay of the fingerprint absorption to a first-order rate law, the charge separation rates (k_{CS}) evolving from ^{1}*C_{60} and the charge recombination rates (k_{CR}) within the $C_{60}^{\bullet-}$−Fc^+ pair were determined with best accuracy—see Tables 1 and 2.

In all cases, no evidence was found for the population of the low-lying ferrocene triplet excited state. This conclusion emerges

from a set of reference experiments with ferrocene (Fc) model compounds. Probing a toluene solution of Fc, for instance, under similar conditions with a 18 ps laser pulse led to very weak absorption changes in the 500−760 nm range. In fact, earlier, an extinction coefficient of less than 500 M^{-1} cm^{-1} was estimated, using laser flash photolysis, for the triplet−triplet absorption in the visible region. The broad and featureless transitions serve as an important reference point, in light of a possible energy transfer process within photoexcited dyads **1**−**6**. In line with the rapid triplet to ground state deactivation (i.e., triplet lifetime of 0.6 ns), we could not detect any appreciable triplet features at time delays exceeding 2 ns.

The kinetic picture of the photoexcited fulleropyrrolidine dyads **1** and **3** will be summarized in the following. In toluene, THF, benzonitrile, and dimethyl formamide (DMF), the fullerene singlet excited state decays significantly faster ($1.7-2.2 \times 10^9$ s^{-1}) than what is seen for the slow ISC dynamics of fulleropyrrolidine reference **7** (5×10^8 s^{-1}). The different ferrocene linkage in dyads **1** and **3**, amidomethyl group in **1** rather than ester group in **3**, improves the donor strength of the Fc moiety in **1** by 0.17 V, increasing the charge transfer energy gap. Despite this energetic difference, kinetic differences are hardly seen. It is important to realize that the flexible bridge most likely induces configurational changes within the donor−acceptor system, either in the ground state or once photoexcited. Consequently, we must assume that the charge separation process is mediated by "through space" interactions between the electron acceptor (C_{60}) and the electron donor (Fc).

Three favorable arguments should be considered, which support these through space interactions. First, the time constants are nearly invariable on the free energy changes. For example, changing the solvent from THF to DMF attenuates the thermodynamic driving force quite substantially from 0.57 to 0.66 eV. Simply, a better solvation of the radical ions is responsible for this thermodynamic effect. This trend was confirmed by complementary fluorescence experiments—see Table 1. Second, it is rather doubtful that the long alkyl chains, which link the donor and the acceptor, would support such an efficient charge separation. Third, despite the clear deactivation of the fullerene singlet excited state, significant nanosecond lifetimes of the charge-separated state were only found in polar solvents. In benzonitrile, values of 130 (7.7×10^6 s^{-1}) and 105 ns (9.5×10^6 s^{-1}) were determined for **1** and **3**, respectively. For comparison, in toluene and THF, no fullerene radical anion features were seen after the conclusion of the 8 ns laser pulse. In fact, in toluene, the fullerene triplet, ^{3}*C_{60}, emerges as the product of this fast charge recombination. In reference to an energetic diagram, we can rationalize this mechanism: While in toluene, the charge-separated radical pair is located above that of the fullerene triplet (1.5 eV),[9] and the better solvation of the radical ions in THF results in lowering the energies (1.16 eV) below that of the triplet. Therefore, the energetics in THF dictate charge recombination back to the singlet ground state, since the triplet population would give rise to an exothermic uphill reaction.

Now we compare fulleropyrrolidinium-based systems **2** and **4**. In dyads **2** and **4**, only the electron acceptor has been modified, meanwhile the electron donors (i.e., amide−Fc and ester−Fc) stayed the same. In principle, the better electron acceptor features of the fulleropyrrolidinium, in which the reduction potential is cathodically shifted by nearly 0.2 V, are expected to affect the intramolecular dynamics.[8b] In fact, relative to **1** and **3**, in both cases, a slightly faster deactivation of the singlet−singlet absorption supports this view.[14] Considering, however, an increase in driving force by nearly 0.2 eV between the fulleropyrrolidine- and the fulleropyrrolidinium-containing ensembles, the differences in deactivation are relatively small (vide supra). Charge recombination reveals a similar relationship, that is, in comparison to **1** and **3** the lifetime of the charge-separated radical pair is hardly prolonged with values of 150 ns (6.6×10^6 s^{-1}) in **2** and 110 ns (9.1×10^6 s^{-1}) in **4**.

It is known that the fullerene surface easily gives rise to through space interactions.[15] Thus, when structurally possible, C_{60}-based ensembles adopt conformations in which the fullerene and the donor moieties assume close proximity to each other. Accordingly, we postulate in dyads **1**−**4** the implication of a rate-determining transition to form the charge transfer-mediating intermediate. To shed light onto the time domain in which these structural rearrangements might take place, we probed the charge separation behavior as a function of solvent viscosity. The lack of changes, noted in a temperature range from 5 to 30 °C, prompts a charge transfer arrangement that is controlled by preorganizations in the ground state.[16] Probably, the most realistic scenario for such an intermediate is an "intramolecular exciplex", in which donor and acceptor have arranged into charge transfer favorable positions. Important for the lifetime of the radical pair is that only solvents, which sufficiently solvate the oppositely charged radical ions, are potent enough to break up this transition state and, in turn, separate the radical cations and radical anions from each other.[15]

If we compare the performance of dyads **1**−**4** in terms of photoinduced electron transfer, we can conclude that fulleropyrrolidinium acceptors accelerate charge separation and stabilize the charged intermediate. However, to demonstrate unambiguously this conclusion, it was necessary to devise and probe dyads **5** and **6** (Scheme 2), whose structural rigidity, provided by an androstane skeleton, dictates only one charge transfer mechanism, namely, "through bond".

The case of the fulleropyrrolidine-based dyad (**5**) transient absorption spectroscopy—carried out in toluene, *ortho*-dichlorobenzene, benzonitrile, and DMF—led to a wide range of deactivation kinetics extending from 6.8×10^8 to 1.4×10^9 s^{-1} (see Figure 4). The overall acceleration is well in accord with a progressively larger ^{1}*C_{60}−Fc/$C_{60}^{\bullet-}$−Fc^+ energy gap, $-\Delta G_{CS}°$, when going from nonpolar (i.e., toluene) to polar environments (i.e., DMF) of up to nearly 1 eV and contrasts the behavior seen for dyads **1** and **3**.[17] In **5**, $C_{60}^{\bullet-}$−Fc^+ is metastable and decays quantitatively to the ground state with lifetimes of 1080 (9.3×10^5 s^{-1}), 820 (1.2×10^6 s^{-1}), and 360 ns (2.8×10^6 s^{-1}) in *ortho*-dichlorobenzene, benzonitrile, and DMF, respectively.[18] If we compare these lifetimes with those summarized for dyads **1** and **3**, we clearly see a stabilization of the radical pair in favor of the rigid spacer. This effect is particularly strong in solvents such as *ortho*-dichlorobenzene, which did not consequence any appreciable stabilization neither for **1** nor for **3**.

For dyad **6**, the charge separation kinetics in *ortho*-dichlorobenzene, benzonitrile, and DMF are all nearly the same. This is surprising, considering the following facts. First, the rigid nature of the spacer locks donor and acceptor into well-defined positions. Second, the variation of $-\Delta G_{CS}°$ is ∼0.3 eV.[19] What is important to note is that the decay kinetics ($\sim 1 \times 10^9$ s^{-1}) are, at least, faster by a factor of 2 than the ISC rates (5×10^8 s^{-1}) found in the reference (**8**). The charge recombination kinetics, on the other hand, in *ortho*-dichlorobenzene (6.2×10^5 s^{-1}), benzonitrile (1.0×10^6 s^{-1}), and DMF (2.0×10^6 s^{-1}) indicate an appreciable acceleration and correlate well with the solvent polarity.

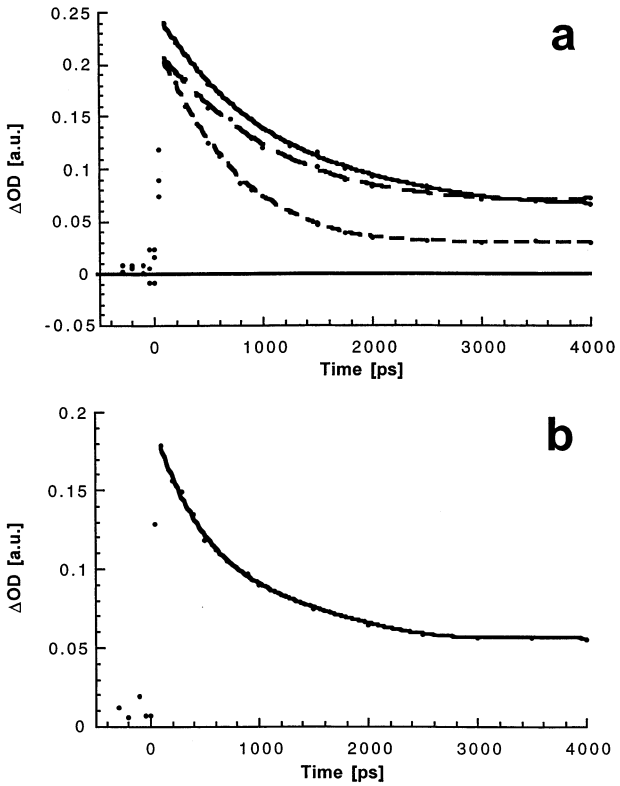

Figure 4. Time−absorption profiles at 880 nm monitoring the fullerene singlet−singlet decay dynamics of (a) dyad **5** in *ortho*-dichlorobenzene (solid line), benzonitrile (dashed line), and DMF (dotted line) and (b) dyad **6** in *ortho*-dichlorobenzene.

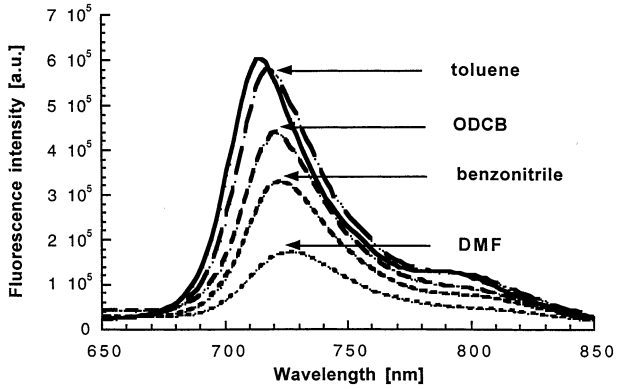

Figure 5. Emission spectra of fulleropyrrolidine **7** reference in toluene (solid line) and dyad **5** in different solvents (see labels for assignment) with matching absorption at the 310 nm excitation wavelength; $OD_{310nm} = 0.8$.

To further follow up on this puzzling observation, steady state and time-resolved fluorescence assays were performed with dyads **5** and **6**. An illustration is given in Figures 5 and 6, which compares the fullerene fluorescence spectra, recorded with matching absorption at the 355 nm excitation wavelength. In principle, tendencies emerge as follows: A clear solvent progression is only seen for dyad **5**, starting with toluene (i.e., strongest C_{60} fluorescence) and ending with DMF (i.e., weakest C_{60} fluorescence), while the quantum yields for dyad **6** in the same solvents are nearly indistinguishable. Also, the C_{60} fluorescence lifetimes in dyad **6**, as determined by the decay of the 720 nm emission maximum, afforded rates on the order of $\sim 1 \times 10^9$ s^{-1}.

Taken all the results into concert, we conclude that the thermodynamic driving force for charge separation in dyad **6**

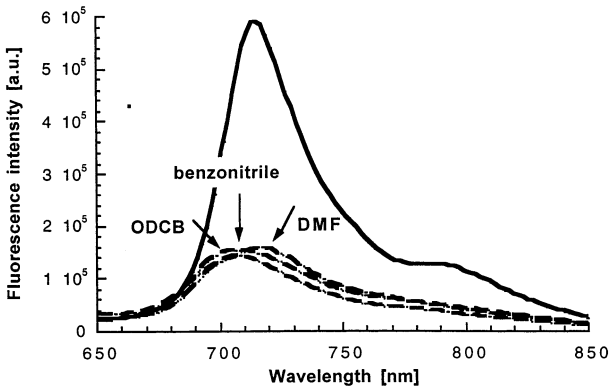

Figure 6. Emission spectra of fulleropyrrolidinium salt **8** reference in THF (solid line) and dyad **6** in different solvents (see labels for assignment) with matching absorption at the 310 nm excitation wavelength; $OD_{310nm} = 0.8$.

must be located in the region close to the top of the Marcus parabola. As a consequence, in dyad **6**, a highly exergonic charge separation prevails with $-\Delta G_{CS}^{\circ} \sim 0.75$ eV, close to the top of the Marcus parabola followed by charge recombination, which is with $-\Delta G_{CR}^{\circ}$ values ~ 1.00 eV clearly in the inverted region of the Marcus parabola, the highly exergonic region ($-\Delta G^{\circ} > \lambda$), where the electron transfer rates start to decrease with increasing free energy changes. An alternative pathway would consider the formation of the zwitterionic $C_{60}^{\bullet -}$ acceptor as the overall rate-determining step. Because parameters associated with the internal, λ_V, and external, λ_S, reorganization energies of C_{60} in charge transfer processes are believed to be similarly small in the investigated solvents,[19] this aspect should also be given some credit.

With the charge separation and charge recombination dynamics in hand, we can now inspect the performance of the fulleropyrrolidine- and fulleropyrrolidinium-based dyads **5** and **6**. For example, the k_{CS} and k_{CR} values in *ortho*-dichlorobenzene were 8.9×10^8 and 9.3×10^5 s^{-1}, respectively, which corresponds to a k_{CS}/k_{CR} ratio of 965 for fulleropyrrolidine dyad **5**. Analogously, a larger ratio of 2340 was estimated for fulleropyrrolidinium dyad **6**. Despite the fact that k_{CR} in both dyads is pushed into the inverted region of the Marcus parabola, it is remarkable that dyad **6**, for which smaller $-\Delta G_{CR}^{\circ}$ values were determined, reveals definitively slower k_{CR}. This points unequivocally to the unique structure of the zwitterionic $C_{60}^{\bullet -}$ acceptor, which provides the means for stabilizing the charge-separated $C_{60}^{\bullet -}-Fc^{+}$ pair.

In the next step, we analyzed the driving force dependence on the rate constants, by applying eq 1, in which V represents the electronic coupling matrix element.

$$k_{ET} = \left(\frac{4\pi^3}{h^2 \lambda k_B T}\right)^{1/2} V^2 \exp\left[-\frac{(\Delta G_{ET}^{\circ} + \lambda)^2}{4\lambda k_B T}\right] \qquad (1)$$

For our current analysis, we transferred eq 1 to a linear expression (i.e., eq 2).

$$k_B T \ln k_{ET} + \frac{\Delta G_{ET}^{\circ}}{2} = k_B T \ln\left[\left(\frac{4\pi^3}{h^2 \lambda k_B T}\right)^{1/2} V^2\right] - \frac{\lambda}{4} - \frac{(\Delta G_{ET}^{\circ})^2}{4\lambda} \qquad (2)$$

The driving forces ($-\Delta G_{ET}^{\circ}$) were determined, based on the first oxidation potential of the ferrocene donor and the first

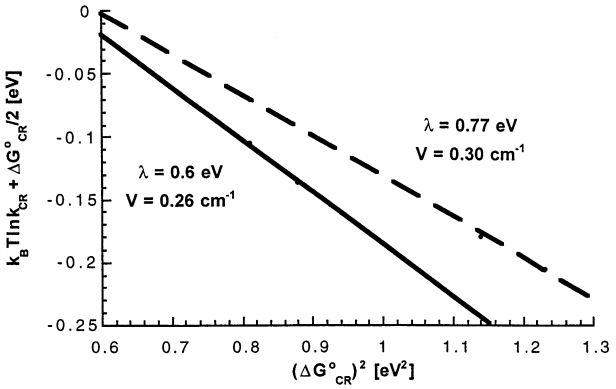

Figure 7. Plot of $[k_BT\ln k_{ET} + (\Delta G_{ET}°/2)]$ vs $(\Delta G_{ET}°)^2$ for dyad **5** (dashed line) and dyad **6** (solid line). The data include the k_{CR} value, and they are taken from Table 3.

TABLE 3: Charge Separation Kinetics in C_{60}−Androstane−Fc Dyad 6 under Variable Conditions

solvent	N_2-saturated (ns)	air-saturated (ns)	O_2-saturated (ns)
ortho-dichlorobenzene	1590	439	125
benzonitrile	965	402	123
DMF	495	261	110

reduction potential of the fulleropyrrolidine and fulleropyrrolidinium acceptors in *ortho*-dichlorobenzene, benzonitrile, and DMF, together with the energy level of the fullerene singlet excited state. In line with eq 2, plots of $[k_BT \ln k_{ET} + (\Delta G_{ET}°/2)]$ vs $(\Delta G_{ET}°)^2$ give for both dyads a linear correlation—see Figure 7. The reorganization energies (λ) and electronic coupling (V) values are obtained for dyad **6** as 0.6 eV and 0.26 cm^{-1}, respectively. A linear correlation was also obtained for **5**, which afforded, however, a larger λ-value (0.77 eV) together with a similar V value (0.3 cm^{-1}). Such a large variance in λ between the fulleropyrrolidine and the fulleropyrrolidinium dyads is the reason the ratio of k_{CS} to k_{CR} is different in the two donor−acceptor systems (Table 2). This is the first quantitative manifestation showing that chemical functionalization helps to control λ-values of a C_{60} electron acceptor.

Finally, the measured oxygen effect deserves special mentioning. In line with our earlier observation regarding $C_{60}^{\bullet-}/Fc^+$ radical pairs, we found no appreciable acceleration of deactivating the charge-separated radical pair, upon saturating benzonitrile and DMF solutions of dyad **5** with either air or molecular oxygen.[20] Dyad **6** shows a different behavior. In the presence of O_2, the decay rate of the $C_{60}^{\bullet-}$ absorption is markedly accelerated as compared to that found in the absence of O_2. Interestingly, the decay rate of $C_{60}^{\bullet-}$ increases linearly with increasing O_2 concentration. The lifetimes in the absence and presence of O_2 for $C_{60}^{\bullet-}-Fc^+$ in dyad **6** in *ortho*-dichlorobenzene, benzonitrile, and DMF are summarized in Table 3. Thus, the presence of the zwitterionic $C_{60}^{\bullet-}$ acceptor appears, without any doubts, essential for the accelerating effect of O_2. Although Fc^+ is spectroscopically invisible in our experiments, we must assume a catalytic function of O_2, since a direct electron transfer from $C_{60}^{\bullet-}$ to O_2 is unlikely to occur, given the fact that the one electron reduction potentials of O_2 is 0.5 V lower than that of C_{60}.

Conclusions

In retrospect, we have demonstrated the beneficial role of a zwitterionic fulleropyrrolidinium acceptor, that is, acceleration of charge separation and deceleration of charge recombination. Central to the stabilization is the small reorganization energy of the fulleropyrrolidinium acceptor, being 0.17 eV smaller than what is found for the analogous fulleropyrrolidine. The favorable electron transfer properties of dyad **6**, that is, a ratio of ~2500 between charge separation and charge recombination, is encouraging to pursue incorporation of **6** into a photovoltaic device via nanoscale organization of photoactive thin films. In particular, the oxygen effect appears critical in (i) contributing to the photocurrent generation and (ii) preventing the oxygen-induced deterioration, usually found in photoactive film materials.

Acknowledgment. This work was supported by the Office of Basic Energy Sciences of the U.S. Department of Energy, MURST (cofin prot. MM2002032171) and C.N.R. through the program "Materiali Innovativi (legge 95/95)". This is contribution NDRL-4442 from the Notre Dame Radiation Laboratory. We thank Dr. Fabio Hollan (CSPA, University of Trieste) for kind help with mass spectrometry.

References and Notes

(1) *J. Mater. Chem.* **2002**, *12*, 1931−2159; special issue on Functionalized Fullerene Materials.

(2) Imahori, H.; Hagiwara, K.; Akiyama, T.; Aoki, M.; Taniguchi, S.; Okada, T.; Shirakawa, M.; Sakata, Y. *Chem. Phys. Lett.* **1996**, *263*, 545. (b) Guldi, D. M.; Asmus, K.-D. *J. Am. Chem. Soc.* **1997**, *119*, 5744. (c) Imahori, H.; Tkachenko, N. V.; Vehmanen, V.; Tamaki, K.; Lemmetyinen, H.; Sakata, Y.; Fukuzumi, S. *J. Phys. Chem. A* **2001**, *105*, 1750.

(3) Haddon, R. C. *Science* **1993**, *261*, 1545.

(4) Prato, M. *J. Mater. Chem.* **1997**, *7*, 1097. (b) Martín, N.; Sánchez, L.; Illescas, B.; Pérez, I. *Chem. Rev.* **1998**, *98*, 2527. (c) Diederich, F.; Gómez-López, M. *Chem. Soc. Rev.* **1999**, *28*, 263. (d) Imahori, H.; Sakata, Y. *Eur. J. Org. Chem.* **1999**, 2445. (e) Reed, C. A.; Bolskar, R. D. *Chem. Rev.* **2000**, *100*, 1075. (f) Fukuzumi, S.; Guldi, D. M. In *Electron Transfer in Chemistry*; Balzani, V., Ed.; Wiley-VCH: Weinheim, 2001; Vol. 2, p 270. (g) Gust, D.; Moore, T. A.; Moore, A. L. *Acc. Chem. Res.* **2001**, *34*, 40.

(5) Guldi, D. M.; Gonzalez, S.; Martin, N.; Anton, A.; Garin, J.; Orduna, J. *J. Org. Chem.* **2000**, *65*, 1978. (b) Guldi, D. M.; Hungerbühler, H.; Carmichael, I.; Asmus, K.-D.; Maggini, M. *J. Phys. Chem. A* **2000**, *104*, 8601. (c) Brabec, C. J.; Cravino, A.; Meissner, D.; Sariciftci, N. S.; Fromherz, T.; Rispens, M. T.; Sanchez, L.; Hummelen, J. C. *Adv. Funct. Mater.* **2001**, *11*, 374. (d) Langa, F.; de la Cruz, P.; Espildora, E.; de la Hoz, A.; Bourdelande, J. L.; Sanchez, L.; Martin, N. *J. Org. Chem.* **2001**, *66*, 5033.

(6) Tamaki, K.; Imahori, H.; Nishimura, Y.; Yamazaki, I.; Shimomura, A.; Okada, T.; Sakata, Y. *Chem. Lett.* **1999**, 227.

(7) Nuber, B.; Hirsch, A. *Acc. Chem. Res.* **1999**, *32*, 795.

(8) Guldi, D. M. *J. Phys. Chem. A* **2000**, *104*, 1483. (b) Da Ros, T.; Prato, M.; Carano, M.; Ceroni, P.; Paolucci, F.; Roffia, S. *J. Am. Chem. Soc.* **1998**, *120*, 11645.

(9) Guldi, D. M.; Prato, M. *Acc. Chem. Res.* **2000**, *33*, 695.

(10) Muller, D.; Zeltser, I.; Bitan, G.; Gilon, C. *J. Org. Chem.* **1997**, *62*, 411.

(11) Kraatz, H.-B. *J. Organomet. Chem.* **1999**, *579*, 222.

(12) Maggini, M.; Scorrano, G.; Prato, M. *J. Am. Chem. Soc.* **1993**, *115*, 9798. (b) Prato, M.; Maggini, M. *Acc. Chem. Res.* **1998**, *31*, 519.

(13) In toluene, no charge separation was found for dyad **5** and the only product was the long-lived fullerene triplet.

(14) Note that the insolubility of **2** and **4** in toluene prevented any experimental comparison.

(15) Guldi, D. M.; Maggini, M.; Scorrano, G.; Prato, M. *J. Am. Chem. Soc.* **1997**, *119*, 974. (b) Guldi, D. M.; Maggini, M.; Scorrano, G.; Prato, M. *Res. Chem. Intermed.* **1997**, *23*, 561.

(16) In fact, similar conclusions were made earlier upon inspecting flexibly spaced C_{60} dyads.

(17) Using the first one electron oxidation potential of the donor ($D^{\bullet+}/D$) and the first one electron reduction potential of the acceptor moiety ($A/A^{\bullet-}$) in *ortho*-dichlorobenzene, benzonitrile, and DMF, the driving forces for the intramolecular charge separation and charge recombination processes were calculated. The Coulombic terms in the present donor−acceptor systems are neglected due to the relatively large edge-to-edge distance (~13.5 Å) and the moderate or high polar solvents employed.

(18) Also in this case, in toluene, no charge separation was found for dyad **5** and the only product is the long-lived fullerene triplet.

(19) Please note that the insolubility given in toluene prevented an experimental comparison.

(20) Fukuzumi, S.; Imahori, H.; Yamada, H.; El-Khouly, M. E.; Fujitsuka, M.; Ito, O.; Guldi, D. M. *J. Am. Chem. Soc.* **2001**, *123*, 2571.